neuroReport

NeuroReport 5, 221–224 (1993)

Ionic basis for intrinsic 40 Hz neuronal oscillations

Xiao-Jing Wang

Department of Mathematics and the James Franck Institute, University of Chicago
5734 S. University Ave.
Chicago, Illinois 60637, USA

We present a biophysical model of a slowly inactivating potassium ion current I_{KS}, based on recent voltage-clamp data from layer V pyramidal neurons in the cat sensorimotor cortex and show that the interplay between a persistent sodium current I_{NaP} and I_{KS} is able to produce intrinsic membrane potential oscillations in the 10- to 50-frequency range. A most notable characteristic of such rhythmicity is what may be termed *mixed-mode bursting*, where clusters of action potentials alternate in time with epochs of small subthreshold oscillations.

Key words: 40 Hz brain rhythm; Biophysical model; Hodgkin–Huxley formalism; Persistent sodium channel; Slowly inactivating potassium channel; Subthreshold oscillation; Clustering of Na^+ spikes; Mixed-mode bursting

Introduction

In recent years evidence has been accumulated that fast, 20–70 Hz ('40 Hz'), rhythmic activity is commonly present in the activated mammalian central nervous system (see Reference 1 for a review). This oscillatory phenomenon occurs concomitantly with arousal, particularly with focused attention and cognition. In field and extracellular unit recordings, as well as in magnetoencephalography, these oscillatory events were seen typically in episodes of short duration (100 to 300 ms), that appeared and disappeared at variable time intervals.[2–10]

Obviously, it is of great interest to look for the cellular origin of this neuronal rhythmicity. Intracellular recordings from cortical and subcortical neurons revealed *subthreshold* membrane potential oscillations at 40 Hz,[11–14] and indicated that intrinsic ion currents may be sufficient to produce such oscillatory activity in some specific neuronal types. In particular, Llinás *et al* reported two subgroups of fast oscillatory neurons in the guinea pig layer IV frontal cortex.[11] One type of neurons displayed rhythmic membrane potentials in a narrow frequency range (35–50 Hz), and was identified as sparsely spinous interneurons on the basis of intracellular staining. The other neuronal type displayed a broader frequency range (10–45 Hz). Since administration of tetrodotoxin (TTX) blocked the oscillatory potentials in both types of cells, it was suggested that a TTX-sensitive persistent sodium conductance (g_{NaP}), in conjunction with a potassium delayed rectifier, would be able to generate such high frequency oscillatory membrane potentials.[11] Among a wide variety of K^+ conductances,[15] however, it remained uncertain what specific type of K^+ conductance was critically involved.

In the present work, the issue of ionic basis for intrinsic 40 Hz membrane potential oscillations is investigated using a computational approach.

Materials and Methods

We shall focus on the interplay between a persistent sodium current and a slowly inactivating potassium current, and discuss a model neuron which is as simple as possible in every other respect. Our model neuron has a single compartment, of which the membrane potential obeys the following equation

$$C_m \frac{dV}{dt} = -g_L(V - V_L) - I_{NaP} - I_{KS} - I_{Na} - I_K + I_{app} \quad (1)$$

where $C_m = 1\ \mu F\ cm^{-2}$, and I_{app} is the injected current (in $\mu A\ cm^{-2}$). The leakage conductance is assumed to be $g_L = 0.1\ mS\ cm^{-2}$, so that the passive time constant $\tau_0 = C_m/g_L = 10$ ms.[16,17]

The four voltage-dependent currents are described by the Hodgkin–Huxley formalism.[18] Thus, a gating variable χ satisfies a first-order kinetics,

$$\frac{d\chi}{dt} = \phi_\chi(\alpha_\chi(V)(1 - \chi) - \beta_\chi(V)\chi) = \phi_\chi(\chi_\infty(V) - \chi)/\tau_\chi(V). \quad (2)$$

For action potential generation we employed the classical Hodgkin–Huxley I_{Na} and I_K, but with higher thresholds. The sodium current $I_{Na} = \bar{g}_{Na} m_\infty^3 h(V - V_{Na})$, where $m_\infty = \alpha_m/(\alpha_m + \beta_m)$, $\alpha_m = -0.1(V + 30 - \sigma)/(\exp(-0.1(V + 30 - \sigma)) - 1)$, $\beta_m = 4\exp(-(V + 55 - \sigma)/18)$; $\alpha_h = 0.07\ \exp(-(V + 44 - \sigma)/20)$, and $\beta_h = 1/(\exp(-0.1(V + 14 - \sigma)) + 1)$. The delayed rectifier $I_K = \bar{g}_K n^4(V - V_K)$, where $\alpha_n = -0.01(V + 34 - \sigma/(\exp(-0.1(V + 34 - \sigma)) - 1)$, and $\beta_n = 0.125\exp(-(V + 44 - \sigma)/80)$. The parameter σ is used for fine tuning the action potential threshold.

The expression of I_{NaP} is taken from Reference 19, described for hippocampal pyramidal cells: $I_{NaP} = \bar{g}_{NaP} m_\infty(V)(V - V_{Na})$, with $m_\infty = 1/(1 + \exp(-(V + 51)/5))$. For both I_{Na} and I_{NaP}, the fast activation variable is substituted by its steady-state function. For the

gating variables h and n, the temperature factor $\phi = 200/7 \approx 28.57$ (corresponding to about 36°C).

We shall choose the I_{KS} described in Reference 20, for layer V pyramidal neurons of cat sensorimotor cortex using an *in vitro* slice preparation and single-electrode voltage-clamp. Adopting a formulation of Huguenard and Prince,[21] I_{KS} is assumed of the following form, $I_{KS} = \bar{g}_{KS} m(\rho h_1 + (1-\rho)h_2)(V - V_K)$, with $\rho = 0.6$. The two inactivation components h_1 and h_2 have a same steady-state function, $h_\infty = 1/(1 + \exp((V + 65)/6.6))$, but disparate time constants. From the experimentally measured inactivation and recovery time constants, we deduced $\tau_{h1} = 200 + 220/(1 + \exp(-(V + 71.6)/6.85))$, and $\tau_{h2} = 200 + 3200/(1 + \exp(-(V + 63.6)/4))$ (see Fig. 1A). The steady-state activation $m_\infty = 1/(1 + \exp(-(V + 34)/6.5))$ (compare Fig. 1B with Fig. 4D of Reference 20). The activation time $\tau_m = 6$ ms was determined by matching the observed time-to-peak of the current evoked by voltage steps, which was found to be not obviously voltage dependent.[20] With this kinetic model of I_{KS}, the voltage-clamp simulations reproduced well the experimental recordings (Fig. 1C). (The time constants for m, h_1 and h_2 are defined at 36°C, with $\phi = 1$). It is worth noting that there seem to exist several variants of I_{KS}, with quantitatively different voltage dependence and sensitivity to tetraethylammonium and 4-aminopyridine. In particular, τ_m of the current described in Reference 21 showed a clear voltage dependence, with a maximum of 22 ms at 36°C. We shall see that the value of τ_m is an important factor in determining the cellular oscillatory properties.

For the simulation results reported below, the following parameter values were used: $\bar{g}_{Na} = 52$, $\bar{g}_K = 20$, $\bar{g}_{NaP} = 0.1$, $\bar{g}_{KS} = 14$ (in mS cm^{-2}); $V_{Na} = +55$, $V_K = -90$, $V_L = -60$ (in mV). The model system was simulated using a fifth-order Runge-Kutta method with adaptive stepsize control and the accuracy parameter $\epsilon = 10^{-5}$ to 10^{-6}.

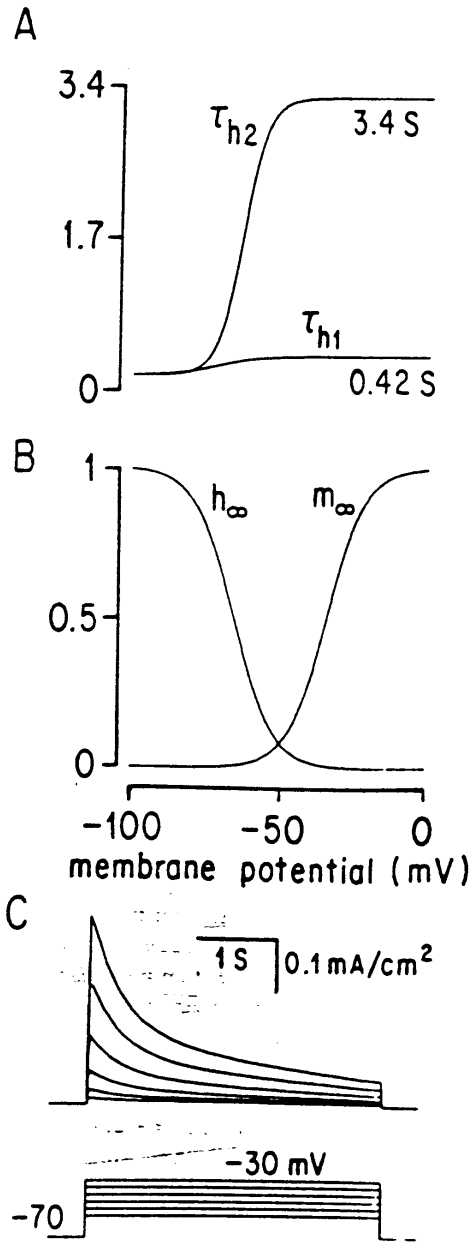

FIG. 1. (A) The inactivation time constants of I_{KS}. τ_m (respectively τ_{h2}) is ~ 420 ms (resp. 3.4 s) for $V > -50$ mV, and converges to 200 ms for $V < -80$ mV. (B) The steady-state activation and inactivation. (C) The current I_{KS} evoked by depolarizing membrane potentials, showing a fast onset and slow decay.

Results

The resting membrane potential was about −66.5 mV. As a constant depolarizing current I_{app} was applied, a subthreshold oscillatory state was observed (Fig. 2A). With increased I_{app} intensity, the oscillation amplitude increased and eventually reached the action potential threshold. The Na^+ spikes were grouped into clusters (bursts), which were interspersed with epochs of subthreshold small oscillations (Fig. 2A); the intra-burst spiking and the inter-burst small waves being of similar frequency. The basic rhythmic frequency was not very sensitive to the I_{app} values, and ranged from 35 to 55 Hz when I_{app} was varied from 0 to 4 μA cm^{-2} (Fig. 2B).

We shall refer to this type of rhythmic activity as *mixed-mode bursting oscillation*. This behavior is similar to that displayed by a mathematical model of bursting in excitable cells by FitzHugh and Rinzel.[22] The alternation between subthreshold waves and clusters of spikes is produced by the slow inactivation kinetics of I_{KS}. As shown in Figure 2C–D, the subthreshold epochs are associated with a gradual decline of the inactivation variable h_1; while the much slower h_2 may be considered as nearly constant. Although during that time the membrane potential does not show obvious depolarization, the accumulated decrease of I_{KS} eventually leads to the elicitation of a cluster of Na^+ spikes. During the repolarization phase of spikes, in the

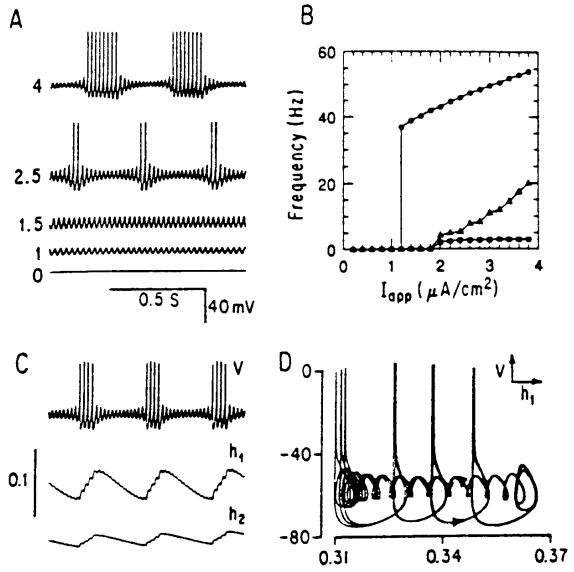

FIG. 2. (A) Membrane potential time courses at various I_{app} values (in μA cm^{-2}), showing transitions from the resting state, to subthreshold oscillation, then to bursting with Na$^+$ spike clusters interspersed with subthreshold oscillatory epochs. (B) The oscillation frequency (circle) is in a narrow range (35–55 Hz for $I_{app} < 4$). The bursting frequency (square) remains remarkably constant (~ 3 Hz), while the spike firing rate (triangle) (equal to the bursting frequency times the number of spikes per burst) increases gradually. The subthreshold oscillatory phase (respectively the burst) is associated with the gradual decrease (resp. increase) of h_1 and h_2 hence of I_{KS}, as can be seen in the time traces (C) and the V-versus-h_1 plot (D) (with $I_{app} = 3$). ($\tau_m = 6$ ms, $\sigma = 0$ mV).

hyperpolarized membrane potential range, I_{KS} de-inactivates (Fig. 2D), until the spike firing ceases and the whole cycle starts over again. According to this scenario, the bursting frequency should be largely determined by the speed of the I_{KS} inactivation process. Indeed, it was found that while both the subthreshold rhythmic frequency and the number of spikes per burst increased with I_{app}, the bursting frequency remained essentially constant (≈ 3 Hz) (Fig. 2B), the period (≈ 330 ms) being comparable with the range of τ_{h1} values (200 to 420 ms).

The basic mechanism underlying the subthreshold oscillation is the interaction between the inward current I_{NaP} and the outward current I_{KS}. As a consequence, the minimal rhythmic frequency is largely determined by the passive time constant τ_0 (or the input resistance), and the I_{KS}-activation time constant τ_m. To illustrate this point, we fixed $\tau_0 = 10$ ms, and significantly increased τ_m (from 6 ms to 50 ms). Then, the minimal rhythmic frequency became 11 Hz, rather than 35 Hz (Fig. 3). In the frequency versus injected current plot (Fig. 3B), there was an initial plateau when the oscillatory patterns were either subthreshold or mixed-mode. This was followed by a gradual increase above 30 Hz, which coincided with the transition to a repetitive spiking state (where every rhythmic cycle was superthreshold).

As expected, the subthreshold oscillatory state was observed only when the spike firing threshold was sufficiently high. When this threshold was lowered by tuning the parameter σ, the first rhythmic regimen emerged from the resting state was no longer purely subthreshold. Instead, it consisted of single Na$^+$ spikes separated by subthreshold oscillations of tiny amplitudes that waxed and waned over a very long time (Fig. 3C). The duration of the subthreshold phases seemed to diverge to infinity (with the bursting frequency going to zero) as the transition between the mixed-mode bursting and the resting state was approached.

Discussion

To summarize, we have shown that the interaction between a persistent sodium current I_{NaP} and a slowly inactivating potassium current I_{KS} presents a suitable ionic mechanism for generating intrinsic 10- to 50-Hz oscillations. A particular K$^+$ channel type with adequate kinetic properties has been identified, and the hypothesis advanced in Reference 11 has been supported. Our study also offered insights into the episodic nature of the 40 Hz neuronal rhythm.

Variations of the I_{NaP} or I_{KS} kinetics, as well as the effects of other types of ion channels, may change quantitatively the precise range of rhythmic frequencies. However, our main theoretical conclusions are expected to remain valid, and should be testable in intracellular recording experiments. First, the rhythmic frequency range is critically dependent on the activation time constant of I_{KS} and the passive time constant. Secondly, the 40 Hz membrane potential rhythm is typically of the mixed-mode bursting form, where clusters of Na$^+$ spikes alternate in time with subthreshold small oscillations. (This feature is conspicuous in the 40 Hz membrane potential oscillations.[11–14]) The bursting frequency is determined by the I_{KS} inactivation rate and is not sensitive to the injected current intensity. And thirdly, if the minimal subthreshold rhythmic frequency is about 10 Hz, the frequency versus injected current plot displays a plateau followed by a smooth increase.

We have shown that while oscillating at 40 Hz, a single cell may be subthreshold for most of the time, and fire action potentials only sparsely (see Fig. 2A, Fig. 3A and Fig. 3C). The underlying cellular property is the I_{KS}-mediated *temporal integration of depolarizations* (this latter has been suggested by Storm,[23] in a context unrelated to rhythmic activities). Therefore, during synchronized 40 Hz population oscillations, individual cells as monitored by extracellular recordings (where subthreshold events are not visible) would display apparently irregular firing and at much lower rate than the field potentials, but their firing would be strongly phase-locked to the population rhythm. Furthermore, since synchronization of neurons in a network depends on the synaptic transmission, the clustering phenomenon of Na$^+$ spikes provides a possible means for the synchrony to occur only *transiently*

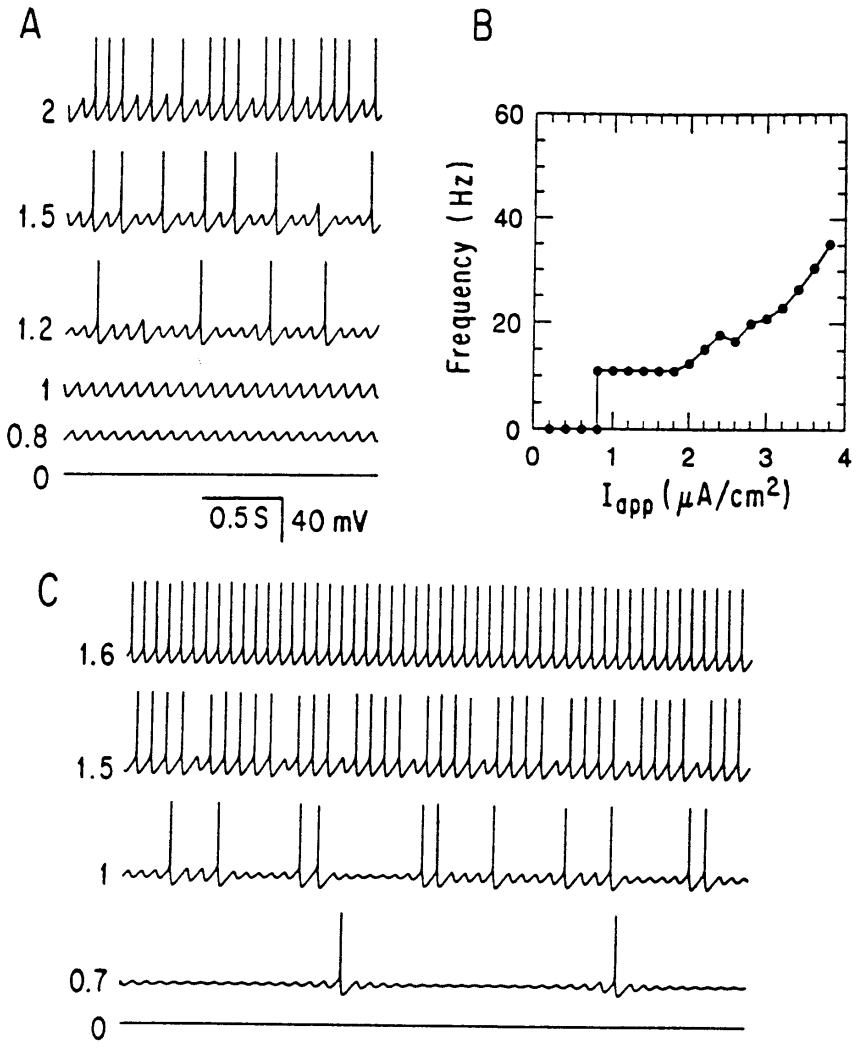

FIG. 3. (A–B) With a larger value of τ_m, the minimal rhythmic frequency is changed to 11 Hz. For $I_{app} \sim 0.8$, the subthreshold oscillation and the mixed-mode oscillation coexist (bistability, not shown). The frequency versus injected current plot displays a plateau followed by a smooth increase. ($\tau_m = 50$ ms, $\sigma = 1$ mV). (C) If the action potential threshold is lowered ($\sigma = -1$ mV), the purely subthreshold oscillatory regimen is absent.

in time. It remains to see if this is relevant to the commonly observed intermittent nature of the synchronized 40 Hz rhythmic events;[2-10] and whether these temporally episodic, cooperative neuronal firing patterns could be dynamical manifestations of cell assemblies in the brain, underlying the serial organization of behavior.

ACKNOWLEDGEMENTS: I thank sincerely Professor L. P. Kadanoff for his kind and continuous support. This work is partly supported by the Office of Naval Research under the contract No. N00014-90J-1194.

Received 25 August 1993; accepted 16 September 1993

References

1. Singer W. *Annu Rev Physiol* 55, 349–374 (1993).
2. Freeman WJ and van Dijk BW. *Brain Res* 422, 267–276 (1987).
3. Eckhorn R, Bauer R, Jordan W *et al. Biol Cybern* 60, 121–130 (1988).
4. Gray CM and Singer W. *Proc Natl Acad Sci USA* 86, 1698–1702 (1989).
5. Gray CM, König P and Engel AK. *Nature (London)* 338, 334–337 (1989).
6. Murthy VN and Fetz EE. *Proc Natl Acad Sci USA* 89, 5670–5674 (1992).
7. Llinás RR and Ribary U. *Proc Natl Acad Sci USA* 90, 2078–2081 (1993).
8. Tiitinen H, Sinkkonen K, Reinikainen K *et al. Nature (London)* 364, 59–60 (1993).
9. Galambos R, Makeig S and Talmachoff PJ. *Proc Natl Acad Sci USA* 78, 2643–2647 (1981).
10. Bouyer JJ, Montaron MF and Rougeul A. *Electroencephalogr Clin Neurophysiol* 51, 244–252 (1981).
11. Llinás RR, Grace AA and Yarom Y. *Proc Natl Acad Sci USA* 88, 897–901 (1991).
12. Pinault D and Deschênes M. *Neuroscience* 51, 245–258 (1992).
13. Nuñez A, Amzica F and Steriade M. *Neuroscience* 51, 7–10 (1992).
14. Mühlethaler M, Khateb A, Fort P *et al. Soc Neurosci Abstr* 18, 197 (1992).
15. Rudy B. *Neuroscience* 25, 729–749 (1988).
16. McCormick DA, Connors BW, Lighthall JW *et al. J Neurophysiol* 54, 782–806 (1985).
17. Mason A and Larkman A. *J Neurosci* 10, 1415–1428 (1990).
18. Hodgkin AL and Huxley AF. *J Physiol (London)* 117, 500–544 (1952).
19. French CR, Sah P, Buckett KJ *et al. J Gen Physiol* 95, 1139–1157 (1990).
20. Spain WJ, Schwindt PC and Crill WE. *J Physiol* 434, 591–607 (1991).
21. Huguenard JR and Prince DA. *J Neurophysiol* 66, 1316–1328 (1991).
22. Rinzel J. A formal classification of bursting mechanisms in excitable cells. Gleason AM, ed. *Proc. Int. Congress of Mathematicians*. Providence, RI: Amer Math Soc, 1987: 1578–1594.
23. Storm JF. *Nature (London)* 336, 379–381 (1988).